Journal of Catalysis 286 (2012) 103–110

Contents lists available at SciVerse ScienceDirect

Journal of Catalysis

journal homepage: www.elsevier.com/locate/jcat

A periodic hybrid DFT approach (including dispersion) to $MgCl_2$-supported Ziegler–Natta catalysts – 1: $TiCl_4$ adsorption on $MgCl_2$ crystal surfaces

Maddalena D'Amore [a,d,*], Raffaele Credendino [a], Peter H.M. Budzelaar [b,d], Mauro Causá [a], Vincenzo Busico [a,c]

[a] Dipartimento di Chimica "Paolo Corradini", Università di Napoli "Federico II", Via Cintia, 80126 Napoli, Italy
[b] Department of Chemistry, University of Manitoba, Winnipeg, Manitoba, Canada R3T 2N2
[c] Department of Chemical Engineering and Chemistry, Eindhoven University of Technology, 5600 MB Eindhoven, The Netherlands
[d] Dutch Polymer Institute, The Netherlands

ARTICLE INFO

Article history:
Received 20 May 2011
Revised 23 September 2011
Accepted 21 October 2011
Available online 29 November 2011

Keywords:
Heterogeneous catalysis
Ziegler–Natta
Dispersion
Density functional theory
M06

ABSTRACT

The adsorption of $TiCl_4$ on the surfaces of $MgCl_2$ crystals has been investigated by means of state-of-the-art periodic hybrid DFT methods, as the first step of a comprehensive study aiming to elucidate the structure of the active species in industrial $MgCl_2$-supported Ziegler–Natta catalysts for ethene and propene polymerization. A first distinctive feature of the approach was the thorough evaluation of dispersion forces, crucial because the binding of $TiCl_4$ on $MgCl_2$ surfaces turned out to be essentially dispersion-driven. Also important was a careful investigation of the effects of different choices on basis set and density functional (DF) on the quantitative aspects of the results; this allowed us to trace the unusually large disagreement in the previous literature and identify unambiguous trends. In particular, three full sets of calculations were run adopting the B3LYP(-D), PBE0(-D) and M06 approximations; to the best of our knowledge, the last represents the first case of M06 functional implementation in a periodic code (CRYSTAL) of widespread use. The results consistently indicated that the adsorption of $TiCl_4$ on well-formed $MgCl_2$ crystals under conditions relevant for catalysis can only occur on $MgCl_2$(1 1 0) or equivalent lateral faces, whereas the interaction with $MgCl_2$(1 0 4) – for decades claimed as the most important surface in stereoselective catalysts – is too weak for the formation of stable adducts. The implications of these findings for catalysis are discussed.

1. Introduction

Although introduced in the polyethylene and polypropylene industry more than 40 years ago with outstanding results, $MgCl_2$-supported Ti-based Ziegler–Natta (ZN) catalysts [1] are still the subject of a controversial debate on the nature and structure of the active species. One way to prepare these catalysts (in the polypropylene version) consists of (i) ball-milling $MgCl_2$, $TiCl_4$ and an 'internal' electron donor (ID), or $MgCl_2$ and the ID alone followed by impregnation of the solid with neat or concentrated $TiCl_4$ at high temperature; (ii) removing the excess $TiCl_4$ and ID by hot-washing with hydrocarbons; and finally (iii) activating the precatalyst by means of a mixture of an Al-trialkyl and an 'external' electron donor (ED). Precatalysts prepared in this way typically contain 1–2% by weight of Ti. The commonly accepted interpretation of this protocol is that $TiCl_4$ adsorbs strongly on certain sites of the $MgCl_2$ surface, stabilized and possibly modulated by the ID, and then remains firmly bound at those sites during subsequent washing, activation and catalysis [1]. More recent preparation routes start from soluble $MgCl_2$/alcohol adducts and end up with precatalysts featuring a well-controlled spherical morphology and a somewhat higher Ti content, but otherwise similar to the ball-milled ones [1,2]. In both cases, based on the properties of the polymers produced, it is safe to conclude that multiple classes of active species are present [1,3]; controlling their distribution is highly desirable, but at the present stage can only be achieved to a limited extent, by means of empirically established choices of the ID (e.g., an aromatic ester or a diether) and ED (e.g., an alkoxysilane) [1].

The unambiguous identification of which $MgCl_2$ surface sites bind $TiCl_4$ and the electron donors strongly enough to survive to the harsh precatalyst preparation would evidently be the starting point for a (more) rational catalyst design and improvement. The present work is part of a comprehensive study aiming at a full elucidation of the local structure of the active surfaces in $MgCl_2$/$TiCl_4$/ID-AlR_3/ED systems. As the first step, here we consider how $TiCl_4$ interacts with $MgCl_2$ in binary $MgCl_2$/$TiCl_4$ adducts, that is where the whole story begins.

* Corresponding author at: Dipartimento di Chimica "Paolo Corradini", Università di Napoli "Federico II", Via Cintia, 80126 Napoli, Italy. Fax: +39 081674057.
E-mail address: mdamore@unina.it (M. D'Amore).

0021-9517/$ - see front matter © 2011 Elsevier Inc. All rights reserved.
doi:10.1016/j.jcat.2011.10.018

Unfortunately, it is very difficult to obtain detailed information from experiments, because these solids are extremely reactive. When crystalline, the platelet-like particles normally offer to the observations the coordinatively saturated basal planes that are of no interest for catalysis. Even the nature of the non-basal $MgCl_2$ surfaces has not been established with certainty. In what is possibly the most relevant surface science experiment on this topic, Magni and Somorjai studied the interaction of $TiCl_4$ with $MgCl_2$ films epitaxially grown on a gold support [4]. They found that at low temperature (<110 K), $TiCl_4$ binds only weakly and is completely removed again on evacuation. If, on the other hand, after condensing $TiCl_4$ on $MgCl_2$ the temperature is first raised to 300 K and then high vacuum is applied, part of $TiCl_4$ is now strongly bound and requires heating to the sublimation temperature of $MgCl_2$ to be removed. The amount of this $TiCl_4$ was estimated as corresponding roughly to 1–2% by weight of Ti, that is close to that found in actual ball-milled catalysts. Somorjai ascribed the strong binding to incorporation into the 'bulk' of $MgCl_2$, without going into details nor discussing the implications for catalysis. Attempts to deposit $MgCl_2$ in the presence of a large excess of $TiCl_4$ were not successful. Based on high-resolution TEM images, Terano reported that small particles in 'activated' crystalline $MgCl_2$samples exhibit, in addition to the basal 001 planes, two kinds of lateral terminations, namely 'atomically flat' 110-type planes and 'atomically rough' planes perpendicular to the former; the adsorption of $TiCl_4$ on $MgCl_2$ severely distorts the crystals and makes their surfaces 'no longer atomically flat planes'[5]. Recent vibrational spectroscopic studies by Zerbi concluded that the surface Ti species are most likely octahedral $TiCl_4$ units on 4-coordinated Mg (e.g., $MgCl_2$(1 1 0) or equivalent planes) [6].

The lack of clear-cut experiments triggered crystallochemical and/or computational modeling approaches. In view of the structural affinity of $MgCl_2$ with 'violet' $TiCl_3$ (the solid precatalyst of first-generation ZN systems [1]), it looked natural to extend to $MgCl_2/TiCl_4$ adducts some fundamental concepts originally developed by Cossee and Arlman for the former [7–9]. The starting assumption is that $TiCl_4$ chemisorption would only take place at coordinatively unsaturated side faces of the platelet-like $MgCl_2$ crystals, such as $MgCl_2$('1 0 0') – more properly $MgCl_2$(1 0 4) – and $MgCl_2$(1 1 0), with 5-coordinated and 4-coordinated Mg atoms, respectively. In particular, according to a pioneering paper by Corradini et al. [10], active species closely mimicking those on authentic $TiCl_3$ surfaces and as such stereoselective in the insertion of propene would result from the epitaxial chemisorption of $TiCl_4$ in the form of dinuclear Ti_2Cl_8 adducts on $MgCl_2$(1 0 4), followed by alkylation and reduction to $Ti_2Cl_{6-y}R_y$ by the AlR_3 co-catalyst (Fig. 1A). The epitaxial chemisorption of $TiCl_4$ on $MgCl_2$(1 1 0), in turn, would ultimately give rise to mononuclear and sterically more open (albeit chiral) $TiCl_2R$ active species (Fig. 1C), claimed to be non-stereoselective in the insertion of propene on the grounds of Molecular Mechanics (MM) calculations. This originated the idea of 'good' and 'bad' $MgCl_2$ crystal faces in polypropylene catalysts, which soon became a common assumption in the literature of the following two decades [1,3,8,11]. Based on qualitative estimates of effective atomic charges, the 'bad' $MgCl_2$(1 1 0) faces were suggested to be more Lewis-acidic than the 'good' $MgCl_2$(1 0 4) faces; as such, they would adsorb Lewis bases (and in particular the ID) more strongly, and in preference to $TiCl_4$ (Fig. 2), which would explain the enhancement of catalyst stereoselectivity by the ID [1,3,8–11].

Much more recently, a number of groups addressed the question by means of Quantum Mechanics (QM) with unexpected and often puzzling results. We carried out a periodic density functional theory (including Dispersion, DFT-D) study of the bulk and surface structures of $MgCl_2$, intended to provide a better-defined picture of the support [12,13]. The main conclusion was that – in the absence of external drivers – well-formed $MgCl_2$ crystals should only feature basal planes and lateral planes with 5-coordinated Mg (e.g., 104 or equivalent for α-$MgCl_2$). The energy of surfaces exposing 4-coordinated Mg (e.g., 110 or equivalent) is high enough that such surfaces should at most constitute a small minority; exposure of Mg sites with even lower coordination seems unlikely except at imperfections (edges, corners, steps). On the other hand, the stability order of different surfaces may change for crystals formed in the presence of adsorbates, as will be discussed in more detail in the following.

Intriguingly, the $TiCl_4$ binding energies to the various $MgCl_2$ surfaces calculated by different groups vary wildly. To one extreme, Martinsky found that adsorption of both mononuclear $TiCl_4$ on $MgCl_2$(1 1 0) and dinuclear Ti_2Cl_8 on $MgCl_2$(1 0 4) is strong [14], which would fit with Corradini's view [10]. To the other extreme, Ziegler concluded *tout court* that there are **no** stable docking sites for $TiCl_4$ on $MgCl_2$ [15]; he proposed that, instead, $TiCl_x$ binds in reduced form, although the nature of the reductant required for this was not specified. Intermediate between these two limits are papers by Parrinello and co-workers [16], Cavallo and co-workers [17], Stukalov et al. [18], Taniike and Terano [19] and others. Most of these conclude that binding is stronger for mononuclear $TiCl_4$ on $MgCl_2$(1 1 0); this is consistent with the aforementioned spectroscopic studies by Zerbi and co-workers [6]. More recent models of active species suggest that surface Ti adducts with a high stereoselectivity in propene insertion may well form on $MgCl_2$(1 1 0) too [20,21].

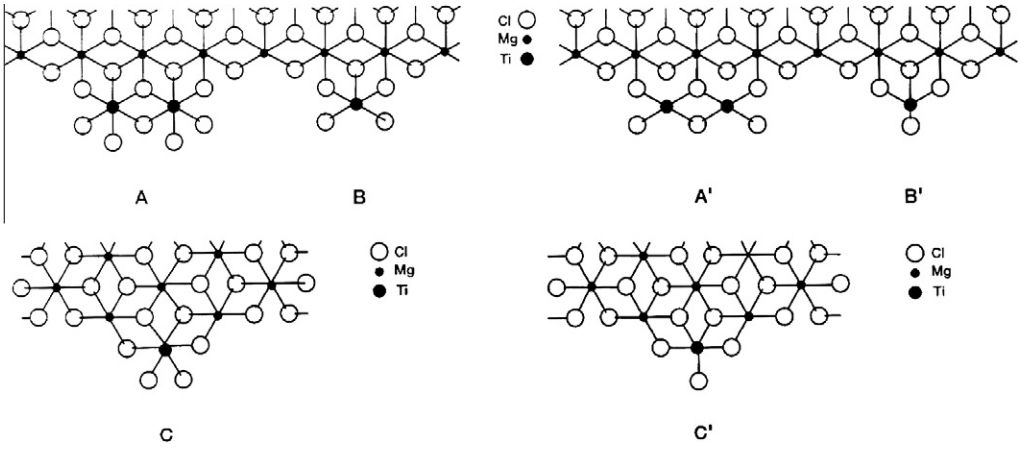

Fig. 1. Epitaxial models of Ti_xCl_{4x} (A–C) and Ti_xCl_{3x} (A′–C′) species on lateral $MgCl_2$ crystal terminations, according to Corradini et al. [10]. Only A′ would evolve to an isotactic-selective active site for polypropylene.

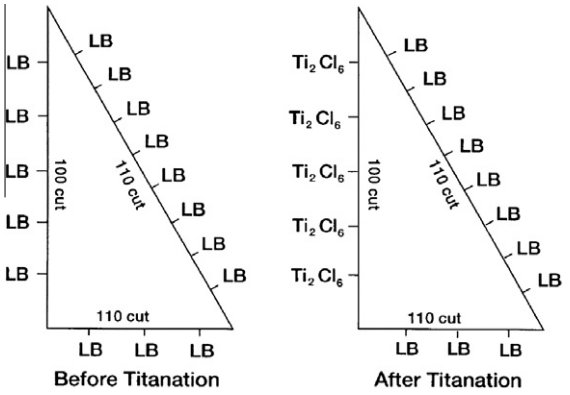

Fig. 2. $MgCl_2$ crystal surface modifications by means of an internal donor according to Corradini et al. [10]. The more acidic $MgCl_2$(1 1 0) cuts would bind the Lewis base (LB) in preference to $TiCl_4$, thus avoiding the formation of non-stereoselective active species (e.g., C′ of Fig. 1).

With this in mind, in the present computational study, we addressed the following questions:

(i) Can we trace the unusually large disagreement in the computational results of $TiCl_4$ binding to $MgCl_2$ reported in the literature?
(ii) Can we produce (more) reliable data?
(iii) Can we reach an unambiguous conclusion on where $TiCl_4$ sits on the surface of $MgCl_2$ and what do the adsorbed species look like?

We adopted a periodic LCAO approach and carefully explored the impact on the computed surface structures and energies of different choices on the density functional (DF), basis set, and treatment of dispersion forces. As we shall see, each of these issues turn out to strongly affect the results, which explains the spread in the earlier literature. Of special importance is the fact that all common generalized gradient approximation (GGA) DF's adopted in DFT calculations, either pure or hybrid, while effectively accounting for correlation in the range of overlapping densities, fail to describe the long-range electron correlations responsible for van der Waals forces [22]. In our previous study of neat $MgCl_2$ [12,13], we noted that including such forces is very important for a correct structural description of this two-dimensional system with weakly bound layers; here we demonstrate that it becomes mandatory when modeling the adsorption of $TiCl_4$ onto $MgCl_2$. For that we considered two basic strategies. One entails a classical correction (of the type $f(R)/R^6$) to the DFT energies and gradients, which were calculated – for comparative purposes – with two well-known hybrid GGA DF's, namely B3LYP [23] and PBE0 [24]; this so-called DFT-D approach [25–27] is very robust, has been applied successfully to literally thousands of very different systems (ranging from rare gas dimers to comparatively large graphene sheets) and is being used more and more in surface science and to address solid state problems [28,29]. The other strategy consists in the adoption of one of the last-generation highly parametrized forms of hybrid meta-GGA DF's, namely the M06 exchange–correlation functional suite [30,31]; designed, inter alia, for application in the area of non-covalent interactions and transition metal bonding, this DF is specially suited to predict structures and energies for systems like the one of interest in the present study.

To perform the latter calculations, we have newly implemented the M06 DF in the CRYSTAL code. It may be worthy to note that CRYSTAL uses a periodic LCAO approach and is a suitable framework for the incorporation of this hybrid functional, whereas periodic codes using plane waves are typically restricted to local DF's (e.g., in the suite of Truhlar DF's, the M06-L lacking the part of exact HF exchange).

To the best of our knowledge, the present is the first thorough attempt to include dispersion interactions in the treatment of $MgCl_2$-supported ZN systems. As we shall see in the following sections, a reasonably good agreement, if not on absolute values at least on trends, was observed between the various methods explored, ending up with chemically significant conclusions on the nature of the $MgCl_2/TiCl_4$ precatalyst. This is important per se, and even more so in view of a future extension of the study to ternary $MgCl_2$/ID/$TiCl_4$ formulations.

2. Computational methods

All calculations were performed with the CRYSTAL09 package, a periodic *ab-initio* program based on atom-centered (Gaussian) basis sets [32]. The surfaces of interest can be modeled in a straightforward manner with the CRYSTAL code by using the slab approach; thin films (2-D infinite systems) with translational symmetry in the hkl planes defining the surfaces are cut out of the previously optimized bulk structure. Before considering the adsorption of Ti_xCl_{4x} species (x = 1 or 2), we checked the convergence of the surface formation energy versus slab thickness, according to the definitions and procedures explained in detail in previous computational studies of neat $MgCl_2$ [13]. The slab thickness necessary for convergence, that is approaching bulk-like behavior in the middle of the slab, turned out to lie in the range of 1.5–2.0 nm (depending on the spacing between the hkl lattice planes considered). As a wide band gap insulator, one might have expected a more rapid convergence of the surface properties (including the formation energy per unit area) versus the number of atomic layers; however, due to the highly ionic nature of $MgCl_2$, the convergence was not so fast.

The adsorption models were built and analyzed keeping the maximum number of symmetry operations; in particular, the up and down symmetry was ensured. The coverage degree ϑ was set at the maximum value compatible with the considered adsorption mode; preliminary tests (see Supplementary Material) demonstrated that decreasing ϑ does not result in appreciable effects on the calculated adsorption energy.

Geometry optimizations were performed in the framework of DFT making use of the hybrid B3LYP, PBE0 and M06 DF's; like for hybrid DF's in general, these include part of the exact HF exchange, which reduces the self-interaction error and improves the performance in the description of the structure of solids.Test calculations adopting the local spin density approximation (LSDA) [33] and pure GGA DF's were also performed (vide infra).

In all calculations, the positions of all atoms were fully relaxed along with the cell parameters. With reference to the CRYSTAL09 user's manual [32], in the evaluation of the Coulomb and Hartree–Fock exchange series, the five threshold parameters (determining the level of accuracy) were set at 7, 7, 7, 7, 14 values. The threshold on the SCF energy was set to 10^{-8} Ha for the geometry optimizations and 10^{-10} Ha for the frequency calculations. The reciprocal space was sampled according to a regular sublattice with shrinking factor equal to 6.

Ti_xCl_{4x} adsorption energies (total electronic energy variations, ΔE_{ads}) were evaluated according to the following formula:

$$\Delta E_{ads} = E_{adduct} - E_{slab} - xE_{TiCl4}$$

where E_{TiCl4} is the electronic energy of the isolated $TiCl_4$ species, E_{slab} is the energy of the bare $MgCl_2$ slab, and E_{adduct} is the energy of the adduct.

In two comparative sets of calculations, we used the B3LYP and PBE0 DF, respectively, either without correcting for dispersion or

computing the dispersion contributions according to the model proposed by Grimme. In the latter case (B3LYP-D and PBE0-D [34]), the DFT energy was semi-empirically corrected by the term:

$$E_{disp} = s_6 \sum_g \sum_{ij} f(R_{ij,g}) \frac{C_6^{ij}}{R_{ij,g}^6}$$

where the summation is over all atom pairs i,j and lattice vectors $\mathbf{g}$ which define the cells of the jth atom, with the exclusion of the $i = j$ contribution for $\mathbf{g} = 0$; C_6^{ij} is the dispersion coefficient for the ijth pair of atoms; f is a damping function used to avoid near-singularities for small inter-atomic distances $R_{ij,\mathbf{g}}$; s_6 is a scaling factor that depends on the adopted DFT method (for B3LYP $s_6 = 1.0$ [27]; for PBE0 $s_6 = 0.6$ [34], as estimated by fitting to the binding energies of non covalently bound complexes belonging in the S22 set [35]).

A third set of calculations was carried out with the M06 DF. Designed by combining the method of constraint satisfaction with parametrization, and optimized against accurate thermochemical and thermal kinetic data to minimize a training function F defined by a sum of root-mean-squared errors, this DF is of special interest to the present work because its reference database includes transition elements, metal–ligand bond energies and non-covalent interactions, also predominantly dispersion-like [30]. Therefore, we decided to implement it in the CRYSTAL code and carry out single-point calculations on the minima previously obtained at DFT-D level of computation. As a check, each minimum was optimized by means of the Gaussian09[36] LCAO code at the M06 level employing periodic boundary conditions; the total number of k points equals to 60 guaranteed convergence on energy.

In all cases, we used a triple-ζ plus polarization quality (TZVP) basis set for Mg, Ti and Cl.[1] Starting from the previously derived 86-411(d31)G [37] for Ti atoms, 86-311G [38] for Cl atoms and 8-511G(d) for Mg atoms [39], the exponents of the outermost and most diffuse Ti and Mg d and Cl sp orbitals were optimized, and an outer d shell was added to better describe the polarization of the Cl atoms. Based on careful tests performed on small clusters with basis sets comprised between the extremes of triple-ζ plus polarization (TZVP [40]) and split-valence with (SVP) polarization [41] quality on all elements, we concluded that the aforementioned choice is a good compromise in terms of accuracy and computational time. We note, in particular, that even a double-ζ plus polarization (DZVP) basis set is unacceptably small for Cl (due to a bad description of its anionic character) and is in fact associated with a strong overestimation of the $TiCl_4$ binding energy compared with the same calculation at TZVP level. In the study of surface phenomena, the incompleteness of basis set determines a non-negligible basis set superposition error (BSSE); the BSSE may partly balance the missing attractive dispersion component, thus yielding structures in fortuitous agreement with experiment. More detailed information on this part is provided as Supplementary Material.

For vibrational analysis, we considered analytical energy gradients with respect to the nuclear positions [42–44], second derivatives were calculated numerically because analytical second derivatives are not yet implemented in CRYSTAL. Within the harmonic approximation, frequencies at the Γ point were obtained by diagonalizing the mass-weighted Hessian matrix W, whose (i,j) element is defined as $W_{ij} = H_{ij}/(M_iM_j)^{1/2}$, where M_i and M_j are the masses of the atoms associated with the i and j coordinates, respectively. The gradients were calculated analytically for all u_j coordinates (u_j being the displacement coordinate with respect to equilibrium), whereas second derivatives at $u = 0$ were obtained by numerical differentiation of the analytical gradients. Since the energy variations corresponding to the displacements considered here can be as small as 10^{-6}–10^{-8} Ha, the SCF cycle needs to be very well converged.

Structures were manipulated and visualized with the MOLDRAW program [45], and molecular drawings were rendered by means of the PovRay program [46] using input files prepared by MOLDRAW.

3. Results and discussions

3.1. Structure and energetics

Experiments and calculations agree that the most stable crystal modification for $MgCl_2$ is the α-form, with space group R-3m [47]. The lattice constants of the conventional hexagonal cell are $\boldsymbol{a}$ = 3.6363(4) Å, $\boldsymbol{c}$ = 17.6663(15) Å, and z_{Cl} = 0.25784(8). As recalled in the Introduction, in our recent B3LYP and B3LYP-D study of α-$MgCl_2$ bulk and surface structures [12,13] we concluded that, in addition to the basal planes (001; 003 when the space group is treated with reference to hexagonal axes, Fig. 3a), well-formed crystals should feature primarily lateral surfaces exposing 5-coordinated Mg atoms (such as the uncharged 104 or equivalent planes, Fig. 3b). The energy of surfaces with four-coordinated Mg atoms (such as the uncharged 110 or equivalent planes, Fig. 3c) was computed to be moderately higher. It is not unreasonable to assume that these planes can form as a result of the extensive mechanical or chemical activation treatments in the presence of adsorbates typical of industrial precatalyst preparations; therefore, we included them in our investigation, in agreement with the original suggestion by Corradini et al. [10].We examined, in particular, mononuclear adsorption of $TiCl_4$ on $MgCl_2(001)$ (which can be described as a physisorption process, in view of the coordinative saturation of Mg on this basal plane), $MgCl_2(104)$ and $MgCl_2(110)$, as well as dinuclear adsorption on $MgCl_2(104)$; the last three cases correspond to those proposed by Corradini as possible precursors of active species (see also Fig. 1) [10,11].

The optimized models are shown in Fig. 4. The corresponding adsorption energies (total electronic energy variations, ΔE_{ads}, as defined in the previous section) computed in the first set of calculations at B3LYP and B3LYP-D level are collected in columns 2 and 3 of Table 1, respectively (coverage degree ϑ corresponding to the maximum achievable value; zero-temperature phonon contributions not taken into account at this stage).

The following facts can be noted:

(i) In at least three out of the four cases considered, ΔE_{ads} is way too low for stable adsorption under conditions representative of catalyst preparation (vide infra). This is even more remarkable if one considers that the data in Table 1 do not include BSSE corrections and that the BSSE of our

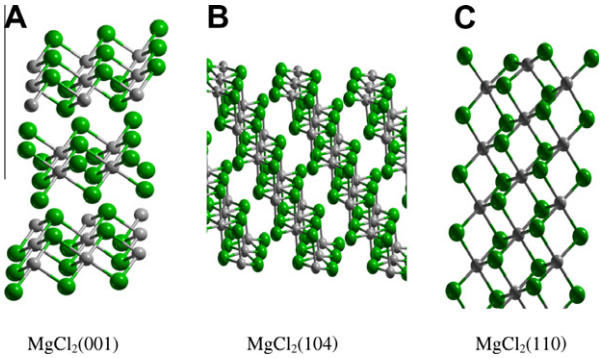

Fig. 3. $MgCl_2(001)$, 6-coordinated Mg; $MgCl_2(104)$, 5-coordinated Mg; $MgCl_2(110)$, 4-coordinated Mg.

[1] The basis on Mg atom is a triple ζ basis set strictly; since this atom is totally ionic, its configuration is [Ne] $3s^0$.

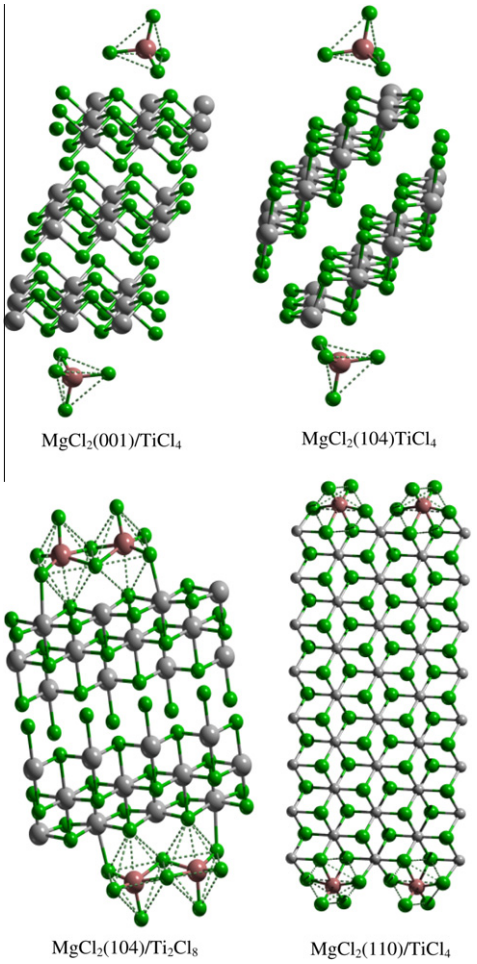

Fig. 4. Selected $MgCl_2(hkl)/Ti_xCl_{4x}$ adsorption minima (optimization performed at B3LYP-D level employing the basis set indicated in the computational section).

Table 1
Values of adsorption energy, ΔE_{ads}, in kcal [mol($TiCl_4$)]$^{-1}$, calculated by means of different DFT(-D) approximations (the adopted basis sets are indicated in the text), for the four $MgCl_2(hkl)/Ti_xCl_{4x}$ adducts of Fig. 4 (for details see text; vibrational zero-point energies not considered).

	B3LYP	B3LYP-D	PBE0-D	M06
$MgCl_2(001)/TiCl_4$ $\vartheta = 1/4$	1.7	−6.1	−9.9	−12.9
$MgCl_2(110)/TiCl_4$ $\vartheta = 1$	−1.6	−15.5	−20.5	−28.6
$MgCl_2(104)/TiCl_4$ $\vartheta = 1/2$	1.3	−7.4	−8.8	−11.9
$MgCl_2(104)/Ti_2Cl_8$ $\vartheta = 2/3$	0.5	−1.4	−5.1	−12.8

optimized triple ζ plus polarization basis sets probably 'inflates' the binding energies by roughly 6 kcal mol^{-1} (as estimated on a sub-system of $MgCl_2(110)/TiCl_4$, see Supplementary Material).

(ii) Comparison of B3LYP and B3LYP-D results provides a striking indication of how important dispersive interactions are in these systems. In fact, applying the dispersion correction increased the calculated ΔE_{ads} values by 2–14 (!) kcal mol $(TiCl_4)^{-1}$ depending on the structure considered; our conclusion therefore is that $TiCl_4$ adsorption is essentially 'dispersion-driven'.

Table 2
Values of standard adsorption free energy, ΔG_{ads}, in kcal [mol($TiCl_4$)]$^{-1}$, calculated by means of different DFT(-D) approximations (the adopted basis sets are indicated in the text), for the four $MgCl_2(hkl)/Ti_xCl_{4x}$ adducts of Fig. 4 (for details see text).

	B3LYP-D		PBE0-D		M06	
	$\Delta G_{ads,g}$	$\Delta G_{ads,l}$	$\Delta G_{ads,g}$	$\Delta G_{ads,l}$	$\Delta G_{ads,g}$	$\Delta G_{ads,l}$
$MgCl_2(001)/TiCl_4$ $\vartheta = 1/4$	5.3	9.2	5.4	9.2	−3.3	0.5
$MgCl_2(110)/TiCl_4$ $\vartheta = 1$	4.1	8.0	−1.9	1.9	−10.3	−6.5
$MgCl_2(104)/TiCl_4$ $\vartheta = 1/2$	5.3	9.2	6.0	9.8	1.3	5.1
$MgCl_2(104)/Ti_2Cl_8$ $\vartheta = 2/3$	15.3	19.1	11.3	15.1	2.3	6.1

(iii) Once adsorbed, the $TiCl_4$ moiety retained its T_d symmetry for $MgCl_2(001)/TiCl_4$ and $MgCl_2(104)/TiCl_4$, whereas the coordination of Ti changed to octahedral for $MgCl_2(110)/TiCl_4$ and $MgCl_2(104)/Ti_2Cl_8$ (Fig. 4). In the last two cases, the calculated structures are very similar to the qualitative models proposed by Corradini in the assumption of a strong epitaxial chemisorption [10] (Fig. 1A and C); however, at least for $MgCl_2(104)/Ti_2Cl_8$, the interaction with the surface is very weak even according to B3LYP-D. MP2 and CCSD(T) calculations by Gordon [48] and our own B3LYP-D ones suggested that the formation of a Ti_2Cl_8 dimer exhibiting D_{3d} symmetry from two $TiCl_4$ molecules corresponds to a shallow energy minimum, whereas the Ti_2Cl_8 dimer with C_{2h} symmetry (the one that an epitaxially chemisorbed species on $MgCl_2(104)$ would possess) was predicted as a transition state in paths for halide exchange between two $TiCl_4$ molecules; evidently, a mild adsorption is enough to induce an epitaxial rearrangement in the structure of the said weakly bound species. For $MgCl_2(104)/TiCl_4$, on the other hand, there is no agreement between the B3LYP(-D) structure (Fig. 4) and that of the hypothetical epitaxially chemisorbed model species (Fig. 1B) [10,11].

As the next step, we calculated at B3LYP-D level the Gibbs free energy of adsorption at 298.15 K and 1.0 atm, ΔG_{ads} for all four models of Fig. 4, with reference to $TiCl_4$ as an ideal gas. We considered harmonic vibrational frequencies and included the contributions to energy and entropy resulting from electronic, vibrational, translational and rotational motions, as well as zero-point and thermal energy corrections. The results are reported in column 2 of Table 2; in column 3, they are added with the experimental value of $\Delta G^{o}_{ev} = 3.836$ Kcal mol^{-1} for the vaporization equilibrium of $TiCl_4$ [49,50], so as to refer them to liquid $TiCl_4$ (which is more relevant to real precatalyst preparation protocols). The separate values of ΔH_{ads} and $T\Delta S_{ads}$ are provided as Supplementary Material.

Based on these estimates, one should conclude that mononuclear TiCl4on $MgCl_2(110)$ is the only case for which the formation of an adduct under standard conditions may be invoked, but even in such a case the binding is – at most – weak. Notably, the most positive value of ΔG_{ads} pertains to $MgCl_2(104)/Ti_2Cl_8$, that is the species suggested by Corradini as the precursor to isotactic-selective active species [10,11]; even if we take the aforementioned dimer instead of two $TiCl_4$ molecules in gas phase as the reference, the value of ΔG_{ads} is highly unfavorable (+10.8 kcal [mol($TiCl_4$)]$^{-1}$ at the B3LYP-D level).

It is important to note at this stage that in DFT-D modeling, a semi-classical dispersion correction of the type $f(R)/R^6$ with a proper scaling (see Section 2) may well represent a general way to handle long-range effects, but different DF's can differ profoundly in the inherent description of medium-range correlations

and therefore end up with different results for highly correlated systems. Although according to Becke [51] the attainment of the exact uniform electron gas limit is a minimal requirement of a functional, a number of popular DF's do not extrapolate correctly to this limit, and yet can perform very well with many atomic and molecular systems. A typical example is that of DF's constructed by recasting the Colle–Salvetti correlation energy formula [52], such as the LYP [53] functional, which can provide a very accurate description of short-range correlations, but miss important longer-range ones that cannot be ignored in extended systems [54]; as such, according to the recent literature, they fail to reproduce the experimental behavior of solids in general, and also of several transition metal–containing systems [55,56]. To the other extreme are the DF's based on the local spin density approximation (LSDA) [57], satisfying the uniform electron gas limit; these include the Perdew series, like P86 [58], PW91 [59], PBE [60], TPSS [61] and PBE0 [24]. All these account better for medium-range correlation effects and seem to perform more satisfactorily in the prediction of thermochemical data [62] at both DFT and DFT-D levels. In recent benchmarking studies [63], PBE0 in particular turned out to provide the best agreement of the calculated properties (including thermochemical ones) with experimental results and CI, CCSD and CCSD(T) computations.

In view of all this, we carried out a second set of DFT-D calculations for the four systems of Table 1 and Fig. 4 using PBE0 instead of B3LYP [64]. The calculated values of ΔE_{ads} and ΔG_{ads} are reported in Tables 1 and 2, respectively; qualitatively, they reproduce the trend highlighted by the B3LYP-D data, but the estimated binding is stronger by up to 5 kcal mol^{-1}. This led, in particular, to predict a negative ΔG_{ads} (=−1.9 kcal mol^{-1}) for the formation of $MgCl_2(1\,1\,0)/TiCl_4$.

We are aware that the reliability of the semi-empirical DFT-D approach as applied to the systems of interest here may be questioned to some extent. Therefore, as explained in the Introduction, we decided to explore an alternative DFT strategy, which entails the use of a last-generation hybrid DF, namely M06, specifically designed and parametrized to describe highly correlated systems featuring transition metals and non-bonded interactions. Starting from the four $MgCl_2(h\,k\,l)/Ti_xCl_{4x}$ geometries optimized at B3LYP-D level, we carried out single-point M06 calculations, with the results reported in the last columns of Tables 1 and 2. The qualitative trends on ΔE_{ads} and ΔG_{ads} are the same of the previous two sets of calculations, but the predicted binding is even stronger than that at PBE0-D level (by 3–8 kcal mol^{-1}, depending on the structure considered). These M06-CRYSTAL results were double-checked by means of optimizations performed using the Gaussian code at M06 level under periodic boundary conditions, ending up with binding energies in quantitative agreement with the CRYSTAL predictions. It is important to note that the geometries of the M06 minima are practically coincident with the PBE0-D ones, which confirms Grimme's conclusion on the excellent performance of the PBE0 functional in this kind of calculations.

Summing up, we believe that the following statements can be made:

(i) It is very likely that the applied DFT and DFT-D methods are close to the limit of what can be achieved in the framework of a 'non-electronic' approach to the computation of dispersive energies. This notwithstanding, and in spite of an unusually large spread of calculated adsorption energies that can be understood in terms of different choices of DF, basis sets and description of long-range electron correlations, it is possible to reach chemically significant conclusions on the structure and energetics of $MgCl_2(h\,k\,l)/Ti_xCl_{4x}$ systems.

(ii) In fact, different methods (with adequate basis sets) agree that the adsorption of $TiCl_4$ on $MgCl_2(1\,0\,4)$, as a mononuclear as well as dinuclear species, is very weak and no stable adducts can be formed under conditions of interest for olefin polymerization catalysis, whereas mononuclear $TiCl_4$ adsorbed on $MgCl_2(1\,1\,0)$ can be proposed as a possible precursor to catalytic species.

(iii) The above disagrees with widely accepted views and interpretations, as will be discussed in the following section.

3.2. Implications for catalysis

If we endorse the conclusions of the previous section, then long-standing hypotheses on the formation of $MgCl_2$-supported Ti-based ZN catalyst systems need to be revised. For over two decades, the beautiful crystallochemical model by Corradini et al. [10] (Figs. 1 and 2) has been looked at as a granitic construction, and most mechanistic proposals – including those on the role(s) of Lewis bases in the modification of the active surfaces – were inspired by/to it [11]. As a matter of fact, when in recent years the first QM studies were published questioning the model as a whole or in part [15,16], the initial reactions were mainly skeptical. However, it is clear now that a number of experimental and theoretical findings are patently inconsistent with the model, particularly with respect to the indication of $MgCl_2(1\,0\,4)$ or equivalent planes with 5-coordinated Mg as the precatalyst surfaces where $TiCl_4$ binds in preference; the present DFT investigation is – we believe – conclusively negative on this point.

The fact that the latter surfaces are predicted to be dominant in well-formed $MgCl_2$ crystals [12,13]and yet cannot fix $TiCl_4$ may appear as an internal contradiction of the emerging DFT(-D) picture. However, one should keep in mind that precatalyst formation occurs under drastic conditions and in the presence of adsorbates ($TiCl_4$ and/or Lewis bases); this can lead to the appearance of $MgCl_2(1\,1\,0)$ (or equivalent) surfaces with 4-coordinated Mg as kinetic products and/or due to stabilization via adsorption. Experimental and computational results supporting such hypotheses have been reported [4–6,12,65–67]; in particular our interpretation of the results by Magni and Somorjai [4] entails the $TiCl_4$-induced reconstruction of $MgCl_2(1\,0\,4)$ into $MgCl_2(1\,1\,0)$.

As also noted in the Introduction, plausible models of isotactic-selective catalytic species for polypropylene on $MgCl_2(1\,1\,0)$ have been proposed by some of us [20] and elaborated upon by others [21]. Therefore, there is no special need to invoke $MgCl_2(1\,0\,4)/Ti_2Cl_8$ as a precursor to stereoselective active sites just because after alkylation and reduction the resulting Ti species would mimic presumed model sites in 'violet' $TiCl_3$ [10]. In particular, even in the absence of Lewis bases, $TiCl_4$ units chemisorbed on $MgCl_2(1\,1\,0)$ at high surface coverage can evolve into moderately isotactic-selective species, because close neighbors at both sides impart the steric hindrance necessary for a chiral orientation of the growing polymer chain according to the classical Corradini's mechanism of stereoselectivity [20].

To validate this view, we prepared by ball-milling a $MgCl_2/TiCl_4$ sample with an average primary particle size of ~11 nm (as estimated from powder X-ray diffraction data), corresponding to ~10% of Mg on lateral crystal terminations, and a Ti loading of 1.74% by weight (Ti/Mg mole ratio ~0.038) [68]. Table 3 summarizes the effects of aging the sample in heptane slurry at 70 °C for 30 min, with or without added $AlEt_3$ and diisobutyldimethoxysilane ($(^iBu)_2Si(OMe)_2$, a typical ED), followed by thorough washings with heptane and pentane and vacuum-drying. In all cases, the Ti content of the solid phase was hardly affected by the aging process; on the other hand, the sample adsorbed appreciable amounts of Al-alkyl and $(^iBu)_2Si(OMe)_2$. Interestingly, the uptake of the latter turned out to be independent of the possible presence

Table 3
Composition of the solid phase recovered after aging the $MgCl_2/TiCl_4$ adduct in heptane slurry at 70 °C for 30 min under different conditions (see text and Supplementary Material).

Aging phase	Ti (%wt)	Al (%wt)	$(({}^{i}Bu)_2Si(OMe)_2$ (%wt)	[Ti]/[Mg]	[Al]/[Mg]	[Si]/[Mg]
None	1.74	0	0	0.038	0	0
Heptane	1.74	0	0	0.038	0	0
Heptane + $AlEt_3$	1.55	0.83	0	0.035	0.033	0
Eptane + $({}^{i}Bu)_2Si(OMe)_2$	1.65	0	2.85	0.037	0	0.015
Heptane + $AlEt_3/({}^{i}Bu)_2Si(OMe)_2$	1.54	0.97	2.73	0.036	0.040	0.015

Table 4
Results of propene polymerization at 70 °C in heptane slurry in the presence of $MgCl_2/TiCl_4$ activated with different co-catalysts (see text and Supplementary Material).[a]

Co-catalyst	R_p[b]	I.I. (%)	$R_{p,iso}$[b,c]	[*mmrrmm*][d]	M_n (kDa)	M_w (kDa)
$AlEt_3$	28.3	26	7.4	1.2	18	82
$AlEt_3$ + $({}^{i}Bu)_2Si(OMe)_2$	6.2	80	5.0	0.4	17	121

[a] Other experimental conditions: $p(C_3H_6)$ = 3.5 bar, $p(H_2)$ = 0.20 bar, [Al]/[Ti] = 150, [Al]/[Si] = 0.20, polymerization time = 60 min.
[b] kg mg (Ti)$^{-1}$ h^{-1} bar^{-1}.
[c] Referred to the 'isotactic' polymer fraction.
[d] Fraction of the *mmrrmm* heptad in the 'isotactic' polymer fraction, as measured from the methyl region of the ^{13}C NMR spectrum.

of $AlEt_3$ in the system, whereas that of the former was always close to equimolar with respect to Ti. Our interpretation of these results is that (a) $TiCl_x$ and $({}^{i}Bu)_2Si(OMe)_2$ adsorb independently on lateral terminations of the $MgCl_2$ crystallites; (b) $AlEt_3$ binds primarily to Ti; (c) practically all Ti is accessible to $AlEt_3$ and hence is located on the $MgCl_2$ crystal surface; (d) the (Ti + Si)/Mg mole ratio (~0.06) points to a high surface coverage.

Results of propene polymerization experiments at 70 °C in heptane slurry in the presence of $MgCl_2/TiCl_4$–$AlEt_3$ and $MgCl_2/TiCl_4$–$AlEt_3/({}^{i}Bu)_2Si(OMe)_2$ systems are summarized in Table 4[68]. As expected [1,3], in the absence of the ED, a poorly stereoregular polypropylene was obtained; in fact, the so-called Index of Isotacticity (I.I.; weight-% insoluble in boiling heptane) was only 26%, and – importantly – the degree of stereoregularity of the 'isotactic' fraction was also comparatively low (~1.2 mol% stereodefects, as measured by ^{13}C NMR). Adding $({}^{i}Bu)_2Si(OMe)_2$ as an ED ([Si]/[Al] = 0.20) enhanced the stereoselectivity with respect to the I.I. (80%) as well as to the average degree of stereoregularity of the 'isotactic' fraction (~0.4 mol% stereodefects); however, these values are well below those achievable for catalyst systems including an ID. Moreover, looking at the catalyst productivity data, it can be concluded that catalyst modification by $({}^{i}Bu)_2Si(OMe)_2$ mainly consisted in the *inhibition* of poorly stereoselective species. It should be recalled that the very same silane ED can yield an appreciable increase in productivity pointing to a *transformation* of poorly stereoselective into highly stereoselective species for catalysts featuring an ID, whenever the latter is removed by reaction with the AlR_3 co-catalyst and replaced by the ED [1,3,11]. In our opinion, all this indicates that the main problem with catalysts derived from binary $MgCl_2/TiCl_4$ adducts is the poor accessibility of part of the $TiCl_x$ adsorbates, which cannot be modified by Lewis base molecules coordinating at vacant surface Mg sites nearby; why this is the case can be easily understood on inspection of Fig. 4.

4. Conclusions and outlook

We carried out a re-visitation by means of state-of-the-art periodic hybrid DFT methods of the long-standing question of $TiCl_4$ adsorption on the surfaces of $MgCl_2$ crystals, as the first step of a comprehensive study aiming to elucidate the structure of the active species in industrial $MgCl_2/TiCl_4/ID\text{-}AlR_3/ED$ ZN catalyst systems for ethene and propene polymerization. The most distinctive and valuable feature of our approach is the inclusion of dispersion contributions in the evaluation of the adsorption energies, mandatory for a correct analysis of the problem because the binding of $TiCl_4$ onto $MgCl_2$ is dominated by such long-range interactions. Also important is the careful investigation of the effects of different choices on DF and basis set on the quantitative aspects of the calculations, which allowed us to trace the unusually large disagreement among previous literature studies and identify unambiguous trends, if not come up with definitive answers.

In brief, our main conclusion is that under conditions representative of $MgCl_2/TiCl_4$ precatalyst preparation $TiCl_4$ can only adsorb on $MgCl_2(1\,1\,0)$ or equivalent lateral faces exposing 4-coordinated Mg. As was discussed in the previous section, this implies that long-standing hypotheses on the genesis of the stereoselective active species for polypropylene and the mechanism(s) of action of the Lewis bases used as selective modifiers must be thoroughly revised.

We believe that our conclusion is sound, both methodologically and because it fits with a number of independent experimental and computational results. On the other hand, one should refrain from over-interpretations. In the first place, in order to validate the DFT(-D) predictions and possibly reduce the error bar of the computations, we will continue the investigation using alternative methods with a different approach to the description of correlation; in particular, in the near future, we plan to adopt a wave-function-based *ab initio method, for example, by carrying out local and/or spin-component-scaled (SCS) MP2 calculations.*

In addition, the computational methods used in this investigation are very demanding, and we are aware that, in spite of the great effort, we did not cover all possible $TiCl_4$ binding modes even for the comparatively simple $MgCl_2/TiCl_4$ system; in particular, adsorption *between* adjacent $MgCl_2$ structural layers (e.g., in the so-called bridging [16] or zipped modes [18]) is a case that remains to be examined, and we will look at it in the continuation of this study. Next, electron donors can alter the relative stability of the surfaces considered here, induce the formation of new ones and even lead to different (possibly amorphous) phases. Moreover, the hypothesis of surface reconstruction entailing the diffusion and partial aggregation of reduced and alkylated $Ti_xCl_{3x-y}R_y$ species cannot be ruled out. Therefore, the identification of the 'docking' surface for $TiCl_4$ adsorption in $MgCl_2/TiCl_4$ adducts is only the first step on the long road to the full understanding of the active sites of ZN catalytic systems.

Acknowledgments

This work is part of the Research Programme of the Dutch Polymer Institute (DPI), Eindhoven, The Netherlands, Project #712. The authors thank Dr. Luca Rongo for the polymerization and precatalyst aging data.

Appendix A. Supplementary material

Supplementary data associated with this article can be found, in the online version, at doi:10.1016/j.jcat.2011.10.018.

References

[1] E. Albizzati, U. Giannini, G. Collina, L. Noristi, L. Resconi, Catalysts and polymerizations, in: E.P. Moore Jr. (Ed.), Polypropylene Handbook, Hanser-Gardner Publications, Cincinnati, OH, 1996 (Chapter 2).
[2] P. Sozzani, S. Bracco, A. Comotti, R. Simonutti, I. Camurati, J. Am. Chem. Soc. 125 (2003) 12881. and refs. therein.
[3] V. Busico, R. Cipullo, Prog. Polym. Sci. 26 (2001) 443.
[4] E. Magni, G.A. Somorjai, Appl. Surf. Sci. 89 (1995) 187.
[5] H. Mori, M. Sawada, T. Higuchi, K. Hasebe, N. Otsuka, M. Terano, Macromol. Rapid Commun. 20 (1999) 245.
[6] L. Brambilla, G. Zerbi, F. Piemontesi, S. Nascetti, G. Morini, J. Mol. Catal. A: Chem. 263 (2007) 103.
[7] (a) P. Cossee, J. Catal. 3 (1964) 80;
(b) E. Arlman, J. Catal. 3 (1964) 89;
(c) E. Arlman, P. Cossee, J. Catal. 3 (1964) 99;
(d) P. Cossee, The mechanism of Ziegler–Natta polymerization. II. Quantum chemical and crystal-chemical aspects, in: A.D. Ketley (Ed.), The Stereochemistry of Macromolecules, vol. 1, Marcel Dekker, New York, 1967, pp. 145–175. Chapter 3, and refs. therein.
[8] P. Corradini, V. Busico, G. Guerra, Comprehensive Polymer Science, vol. 4, Pergamon Press, Oxford, 1988, pp. 29–50.
[9] (a) U. Giannini, Makromol. Chem. Suppl. 5 (1981) 216;
(b) U. Giannini, G. Giunchi, E. Albizzati, P.C. Barbè, in: M. Fontanille, A. Guyot (Eds.), Proc. NATO ASI Sect, vol. 215, D. Reidel Publishing, Dordrecht, 1987, p. 473.
[10] P. Corradini, V. Barone, R. Fusco, G. Guerra, Gazz. Chim. Ital. 113 (1983) 601.
[11] (a) V. Busico, P. Corradini, L. De Martino, A. Proto, V. Savino, E. Albizzati, Makromol. Chem. 186 (1985) 1279;
(b) V. Busico, P. Corradini, L. De Martino, A. Proto, E. Albizzati, Makromol. Chem. 187 (1986) 1115;
(c) V. Busico, P. Corradini, A. Ferraro, Makromol. Chem. 187 (1986) 1125;
(d) V. Busico, P. Corradini, L. De Martino, F. Graziano, A. Iadicicco, Makromol. Chem. 192 (1991) 49;
V. Busico, R. Cipullo, P. Corradini, R. De Biasio, Macromol. Chem. Phys. 196 (1995) 491;
(e) E. Albizzati, U. Giannini, G. Morini, G. Galimberti, L. Barino, R. Scordamaglia, Makromol. Chem., Macromol. Symp. 89 (1995) 73;
(f) L. Barino, R. Scordamaglia, Makromol. Chem., Macromol. Symp. 89 (1995) 101.
[12] V. Busico, M. Causà, R. Cipullo, R. Credendino, F. Cutillo, N. Friederichs, R. Lamanna, R.; A. Segre, V. Van Axel Castelli, J. Phys. Chem. C 112 (2008) 1081.
[13] R. Credendino, V. Busico, M. Causà, V. Barone, P.H.M. Budzelaar, C. Zicovich-Wilson, Phys. Chem. Chem. Phys. 11 (2009) 6525.
[14] C. Martinsky, C. Minot, J.M. Ricart, Surface Sci. 490 (2001) 237.
[15] M. Seth, P.M. Margl, T. Ziegler, Macromolecules 35 (2002) 7815.
[16] (a) M. Boero, M. Parrinello, K. Terakura, J. Am. Chem. Soc. 120 (1998) 2746;
(b) M. Boero, M. Parrinello, S. Hüffer, H. Weiss, J. Am. Chem. Soc. 122 (2000) 501;
(c) M. Boero, M. Parrinello, H. Weiss, S. Hüffer, J. Phys. Chem. A 105 (2001) 5096.
[17] (a) G. Monaco, M. Toto, G. Guerra, P. Corradini, L. Cavallo, Macromolecules 33 (2000) 8953;
(b) N. Bahri-Laleh, A. Correa, S. Mehdipour-Ataei, H. Arabi, M.N. Haghighi, G. Zohuri, L. Cavallo, Macromolecules 44 (2011) 778.
[18] D.V. Stukalov, I.L. Zilberberg, V.A. Zakharov, Macromolecules 42 (2009) 8165.
[19] T. Taniike, M. Terano, Macromol. Rapid Commun. 29 (2008) 1472.
[20] (a) V. Busico, R. Cipullo, G. Monaco, G. Talarico, M. Vacatello, J.C. Chadwick, A.L. Segre, O. Sudmeijer, Macromolecules 32 (1999) 4173;
(b) V. Busico, R. Cipullo, C. Polzone, G. Talarico, J.C. Chadwick, Macromolecules 36 (2003) 2616;
(c) V. Busico, J.C. Chadwick, R. Cipullo, S. Ronca, G. Talarico, Macromolecules 37 (2004) 7437.
[21] A. Correa, F. Piemontesi, G. Morini, L. Cavallo, Macromolecules 40 (2007) 9181.
[22] A. Ruzsinszky, J.P. Perdew, G.I. Csonka, J. Phys. Chem. A 109 (2005) 11015.
[23] A.D. Becke, J.Chem Phys. 98 (1993) 5648.
[24] C. Adamo, V. Barone, J. Chem. Phys. 110 (1999) 6158.
[25] S. Grimme, J. Comput. Chem. 25 (2004) 1463.
[26] S. Grimme, J. Comput. Chem. 27 (2006) 1787.
[27] B. Civalleri, C.M. Zicovich-Wilson, L. Valenzano, P. Ugliengo, CrystEngComm 9 (2007) 1.
[28] K.E. Yousaf, E.N. Brothers, J. Chem. Theory Comput. 6 (2010) 864.
[29] F. Shimojo, Z. Wu, A. Nakano, R.K. Kalia, P. Vashista, J. Chem. Phys. 132 (2010) 094106.
[30] Y. Zhao, D.G. Truhlar, Theor. Chem. Account. 120 (2008) 215.
[31] Y. Zhao, N.E. Schultz, D.G. Truhlar, J. Chem. Theory Comput. 2 (2006) 364.
[32] R. Dovesi,V.R. Saunders, R. Orlando, C.M. Zicovich-Wilson, F. Pascale, B. Civalleri, K. Doll, I.J. Bush, P. D'Arco, M. Lunell, Crystal 2009 User Manual, Turin University, Turin.
[33] S.H. Vosko, L. Wilk, M. Nusair, Can. J. Phys. 58 (1980) 1200.
[34] R. Huenerbein, B. Schirmer, J. Moellmann, S. Grimme, Phys. Chem. Chem. Phys. 12 (2010) 6940.
[35] P.Jurečka,J.Šponer,J.Černy,P.Hobza,Phys.Chem.Chem.Phys.8(2006)1985–1993.
[36] M.J. Frisch, G.W. Trucks, H.B. Schlegel, G.E. Scuseria, M.A. Robb, J.R. Cheeseman, G. Scalmani, V. Barone, B. Mennucci, G.A. Petersson, H. Nakatsuji, M. Caricato, X. Li, H.P. Hratchian, A.F. Izmaylov, J. Bloino, G. Zheng, J.L. Sonnenberg, M. Hada, M. Ehara, K. Toyota, R. Fukuda, J. Hasegawa, M. Ishida, T. Nakajima, Y. Honda, O. Kitao, H. Nakai, T. Vreven, J.A. Montgomery, Jr., J.E. Peralta, F. Ogliaro, M. Bearpark, J.J. Heyd, E. Brothers, K.N. Kudin, V.N. Staroverov, R. Kobayashi, J. Normand, K. Raghavachari, A. Rendell, J.C. Burant, S.S. Iyengar, J. Tomasi, M. Cossi, N. Rega, J.M. Millam, M. Klene, J.E. Knox, J.B. Cross, V. Bakken, C. Adamo, J. Jaramillo, R. Gomperts, R.E. Stratmann, O. Yazyev, A.J. Austin, R. Cammi, C. Pomelli, J.W. Ochterski, R.L. Martin, K. Morokuma, V.G. Zakrzewski, G.A. Voth, P. Salvador, J.J. Dannenberg, S. Dapprich, A.D. Daniels, Ö. Farkas, J.B. Foresman, J.V. Ortiz, J. Cioslowski, D.J. Fox, Gaussian 09, Revision A.1, Gaussian, Inc., Wallingford CT, 2009.
[37] F. Cora, Mol. Phys. 103 (2005) 2483.
[38] E. Apra, M. Causa', M. Prencipe, R. Dovesi, V.R. Saunders, J. Phys. Condens. Matter 5 (1993) 2969.
[39] L. Valenzano, Y. Noel, R. Orlando, C.M. Zicovich-Wilson, M. Ferrero, R. Dovesi, Theor. Chem. Acc. (2006), doi:10.1007/s00214-006-0213-2.
[40] A. Schäfer, C. Huber, R. Ahlrichs, J. Chem. Phys. 100 (1994) 5829.
[41] A. Schäfer, H. Horn, R. Ahlrichs, J. Chem. Phys. 97 (1992) 2571.
[42] K. Doll, N.M. Harrison, V.R. Saunders, Int. J. Quantum Chem. 82 (2001) 1.
[43] K. Doll, Comput. Phys. Commun. 137 (2001) 74.
[44] F. Pascale, C.M. Zicovich-Wilson, R. Orlando, C. Roetti, P. Ugliengo, R. Dovesi, J. Phys. Chem B 109 (2005) 6146–6152.
[45] Moldraw Program, P. Ugliengo, G. Chiari, <http://www.chimifm.unito.it/fisica/moldraw/moldraw.html>.
[46] PovRay Persistence of Vision Pty. Ltd. Persistence of Vision (TM) Raytracer. Persistence of Vision Pty. Ltd., Williamstown, Victoria, Australia, 2004. <http://www.povray.org/>.
[47] D.E. Partin, ; M. O'Keeffe, J. Solid State Chem. 95 (1991) 176.
[48] S.P. Webb, M.S. Gordon, J. Am. Chem. Soc. 121 (1999) 2552.
[49] NIST Chemistry WebBook: webbook.nist.gov/chemistry.
[50] (a) Selected values of Chemical Thermodynamic Properties, in: D.D. Wagman (Ed.), National Bureau of Standards, July 1, 1953;
(b) K.K. Kelley, The entropies of inorganic substances, US Bur. Mines Bull. (1941) 434.
[51] A.D. Becke, J. Chem. Phys. 104 (1996) 1040.
[52] R. Colle, D. Salvetti, Theor. Chim. Acta 37 (1975) 329.
[53] C. Lee, W. Yang, R.G. Parr, Phys. Rev. B 37 (1988) 785.
[54] J. Tao, P. Gori-Giorgi, J.P. Perdew, R. McWeeny, Phys. Rev. A 63 (2001) 032513.
[55] D.A. Pantazis, J.E. Mc Grady, F. Maseras, M. Etienne, J. Chem.Theory Comput. 3 (2007) 1329.
[56] S. Zhao, Z.H. Li, W.N. Wang, Z.P. Liu, K.N. Fan, J. Chem. Phys. 124 (2006) 184102.
[57] S.H. Vosko, L. Wilk, M. Nusair, Can. J. Phys. 58 (1980) 1200.
[58] J.P. Perdew, Phys. Rev. B. 33 (1986) 8822.
[59] J.P. Perdew, J.A. Chevary, S.H. Vosko, K.A. Jackson, M.R. Pederson, D.J. Singh, C. Fiolhais, Phys. Rev. B 46 (1992) 6671;
J.P. Perdew, K. Burke, Y. Wang, Phys. Rev. B 54 (1996) 16533.
[60] J.P. Perdew, K. Burke, M. Ernzerhof, Phys. Rev. Lett. 77 (1996) 3865;
J.P. Perdew, K. Burke, M. Ernzerhof, Phys. Rev. Lett. 78 (1997) 1396.
[61] J. Tao, J.P. Perdew, V.N. Staroverov, G.E. Scuseria, Phys. Rev. Lett. 91 (2003) 146401;
J.P. Perdew, J. Tao, V.N. Staroverov, G.E. Scuseria, J. Chem. Phys. 120 (2004) 6898.
[62] S. Grimme, J. Antony, S. Ehrlich, H. Krieg, J. Chem. Phys. 132 (2010) 154104.
[63] R. Huenerbein, B. Schirmer, J. Moellmann, S. Grimme, Phys. Chem. Chem. Phys. 12 (2010) 6940.
[64] This is part of a systematic investigation on the impact of different DF's on the DFT-D modeling of ZN catalysts, as will be reported in a separate manuscript.
[65] A. Turunen, M. Linnolahti, V.A. Karttunen, T.A. Pakkanen, P. Denifl, T. Leinonen, J. Mol. Catal. A: Chem. 334 (2011) 103.
[66] R. Credendino, J.T.M. Pater, A. Correa, G. Morini, L. Cavallo, J. Phys. Chem. C 115 (2011) 13322.
[67] A. Andoni, J.C. Chadwick, H.J.W. Niemantsverdriet, P.C. Thüne, Macromol. Rapid Commun. 28 (2007) 1466.
[68] For experimental details, see Supplementary Material.